J Therm Anal Calorim (2012) 108:371–379
DOI 10.1007/s10973-011-1866-1

Thermal and spectroscopic studies on solid Ketoprofen of lighter trivalent lanthanides

D. A. Gálico · B. B. Holanda · G. L. Perpétuo · E. Schnitzler · O. Treu-Filho · G. Bannach

Received: 25 July 2011 / Accepted: 10 August 2011 / Published online: 3 September 2011

Abstract Solid-state $Ln(L)_3$ compounds, where Ln stands for trivalent La, Ce, Pr, Nd, Sm, Eu, and L is ketoprofen have been synthesized. Thermogravimetry (TG), differential thermal analysis (DTA), differential scanning calorimetry (DSC) as well as X-ray diffraction powder (DRX) patterns, Fourier transformed infrared spectroscopy (FTIR), and other methods of analysis were used to study solid Ketoprofen of lighter trivalent lanthanides. The results provided information of the composition, dehydration, coordination mode, structure, thermal behavior, and thermal decomposition. The theoretical and experimental spectroscopic study suggests that the carboxylate group of ketoprofen is coordinate to metals as bidentate bond.

Keywords Ketoprofen · Thermal behavior · Infrared spectroscopy · Carboxylate coordination

Introduction

Thermal methods of analysis are widely used for checking thermal decomposition, thermal stability [1–4], polymorphism [1], reactions in solid state, drug formulations [5–7], purity [8], evolved gas analysis using simultaneous TG–FTIR [9] and other properties of solid compounds used in pharmaceutical industry [10]. DSC was used as a screening technique to determine the compatibility of ketoprofen with excipients [11], as well as theoretical calculations in structural investigations [3]. Owing to the numerous issues involved, it becomes important to have a complete understanding of the properties of pharmaceutical materials.

The Ketoprofen is a nonsteroidal anti-inflammatory agent that belongs to the class of 2-arylpropionic acids which constitute a considerable group of pharmaceutical and commercial interest. From the pharmacological standpoint, the 2-arylpropionic acids act by blocking the conversion of arachidonic acid into prostaglandins and thromboxane A2, responsible for the inflammatory mechanism through inhibition of cyclooxygenase [12].

The lanthanides show widely diverse coordination compounds. These compounds often possess remarkable and unique spectroscopic properties, photophysical, and electrochemical applications can be explored in sensory, pharmacological, and diagnostic [13–16].

The motivation for the preparation of lanthanide complexes with ketoprofen is the structural similarity with other lanthanide complexes already reported in the literature, that show pharmacological, diagnostic, and therapeutic applications [16]. So this study can contribute as a basis for future pharmacological applications.

Experimental

The ketoprofen (acid form) with ≥98% purity was obtained from Aldrich. Aqueous solution of ketoprofen sodium salt

D. A. Gálico · B. B. Holanda · G. L. Perpétuo · G. Bannach (✉)
Departamento de Química, Falculdade de Ciências, UNESP, Bauru, SP CEP 17033-260, Brazil
e-mail: gilbert@fc.unesp.br

E. Schnitzler
Universidade Estadual de Ponta Grossa, Depto. Química, Ponta Grossa, PR CEP 84030-900, Brazil

O. Treu-Filho
Instituto de Química, UNESP, Araraquara, SP CEP 14800-900, Brazil

(0.1 mol L^{-1}) was prepared by neutralization aqueous ketoprofen suspension with 0.1 mol L^{-1} sodium hydroxide solution and the pH was adjusted to 8.0. The 3D theoretical structure of ketoprofen is showed in Fig. 1.

Lanthanide chlorides were prepared from the corresponding metal oxides (except for cerium) by treatment with concentrated hydrochloric acid. The resulting solutions were evaporated to near dryness, the residues redissolved in distilled water and the solutions again evaporated to near dryness to eliminate the excess of hydrochloric acid. The residues were again dissolved in distilled water, transferred to a volumetric flask and diluted in order to obtain ca. 0.1 mol L^{-1} solutions, whose pH were adjusted to 5.0 by adding diluted sodium hydroxide or hydrochloric acid solutions. Cerium (III) was used as its nitrate and ca. 0.1 mol L^{-1} aqueous solutions of this ion were prepared by direct weighing and dissolution of the salt.

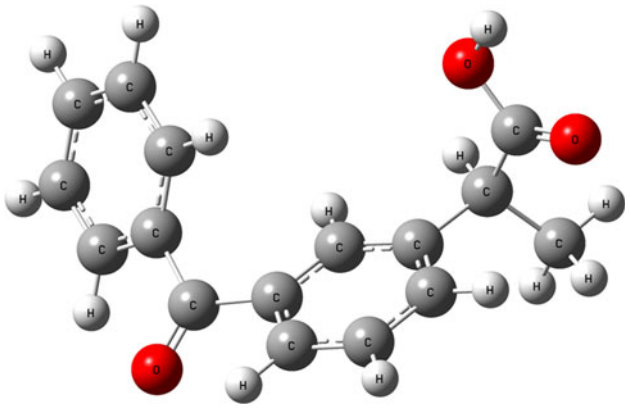

Fig. 1 3D theoretical structure of ketoprofen (optimized using DFT/B3LYP method)

Solid state compounds were prepared by adding slowly with continuous stirring, solutions of ketoprofen sodium salt to the respective metal chloride or nitrate solutions, until total precipitation of metal ions. The precipitates were washed with distilled water in order to elimination of chloride (or nitrate) ions, filtered through and dried on Whatman no. 42 filter paper, and kept in a desiccator over anhydrous calcium chloride.

Simultaneous TG–DTA curves were obtained with thermal analysis system, model SDT 2960 (TA Instruments). The purge gas was an air flow of 100 mL min^{-1}. A heating rate of 20 °C min^{-1} was adopted, with samples weighing about 5 mg. Alumina crucible was used for TG–DTA curves.

The metal ions were also determined by complexometric titrations with standard EDTA solution, using xylenol orange as indicator [17].

Table 1 Analytical data for $Ln_2L_3{\cdot}nH_2O$

Compound	Metal/%			Δ_{Ligand}/%		Water/%		Filial residue/%		
	Calc.	TG	EDTA	Calc.	TG	Calc.	TG	Calc.	TG	Oxide
$La(L)_3{\cdot}lH_2O$	15.15	15.10	15.94	80.26	80.12	1.97	2.17	17.77	17.71	La_2O_3
$Ce(L)_3{\cdot}1.5H_2O$	15.13	15.17	15.93	78.51	78.32	2.92	3.06	18.57	18.62	CeO_2
$Pr(L)_3{\cdot}0.5H_2O$	15.49	15.35	15.96	80.30	81.01	0.99	1.06	18.71	17.93	Pr_6O_{11}
$Nd(L)_3{\cdot}1.5H_2O$	15.49	15.74	16.15	79.03	78.68	2.90	2.88	18.07	18.44	Nd_2O_3
$Sm(L)_3{\cdot}0.5H_2O$	16.36	15.38	16.52	80.05	81.15	0.98	1.02	18.97	17.83	Sm_2O_3
$Eu(L)_3{\cdot}lH_2O$	16.35	16.46	16.53	79.14	78.66	1.94	2.34	18.92	19.00	Eu_2O_3

L ketoprofen

Table 2 IR spectroscopic data for sodium ketoprofen and for its compounds with lighter bivalent lanthanides

Compound	ν_{O-H}/cm^{-1}	$\nu_{anti\text{-}sym(COO)^-}/cm^{-1}$	$\nu_{sym(COO)^-}/cm^{-1}$	$\nu_{C=O}/cm^{-1}$	Δ/cm^{-1}
$NaL{\cdot}1H_2O$	3400	1567	1394	1660, 1645	173
$La(L)_3{\cdot}lH_2O$	3400	1548	1409	1658	139
$Ce(L)_3{\cdot}1.5H_2O$	3400	1547	1409	1658	138
$Pr(L)_3{\cdot}0.5H_2O$	3400	1547	1410	1658	137
$Nd(L)_3{\cdot}1.5H_2O$	3400	1545	1414	1658	131
$Sm(L)_3{\cdot}0.5H_2O$	3400	1547	1414	1658	133
$Eu(L)_3{\cdot}lH_2O$	3400	1547	1415	1658	132

L ketoprofen, ν_{O-H} hydroxyl group stretching frequency, $\nu_{anti-sym\cdot(COO^-)}$and $\nu_{sym(COO^-)}$ symetiical and anti-symetiical vibrations of the COO^- group, respectively. $\nu_{c=o}$ ketonic carbonyl stretching frequency, $\Delta\ \nu_{anti-sym(COO^-)}]-[\nu_{sym(COO^-)}]$

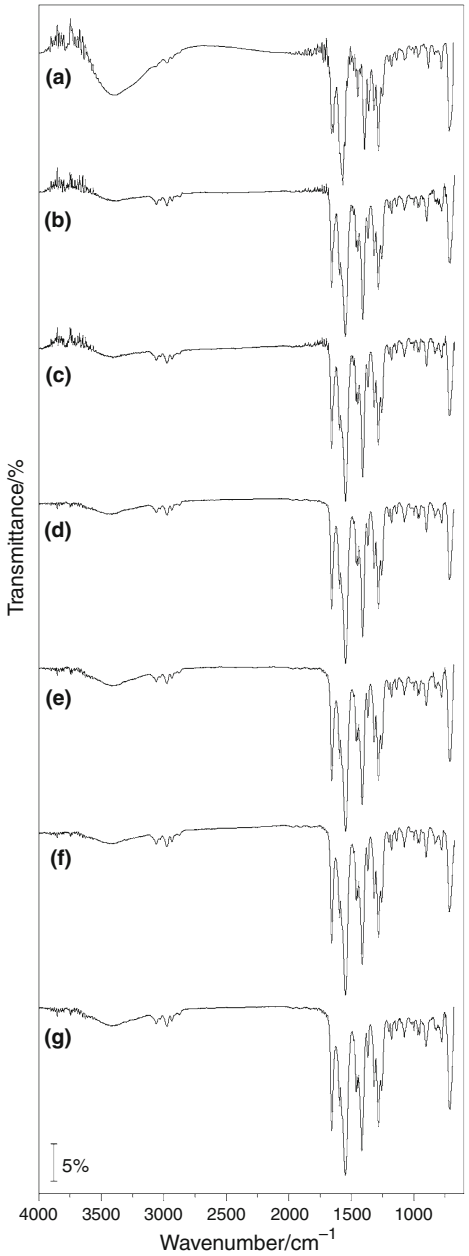

Fig. 2 Attenuate total reflectance infrared spectra of **a** NaL·1H_2O, **b** La$(L)_3$·1H_2O, **c** Ce$(L)_3$·1.5H_2O, **d** Pr$(L)_3$·0.5H_2O, **e** Nd$(L)_3$·1.5H_2O, **f** Sm$(L)_3$·0.5H_2O, **g** Eu$(L)_3$·1H_2O

DSC curves were obtained with thermal analysis systems model Q-10 (TA Instruments). The purge gas was an air flow of 100 mL min^{-1}. A heating rate of 20 °C min^{-1} was adopted with samples weighing about 3 mg. Aluminum crucibles, with perforated cover, were used for recording the DSC curves.

X-ray powder patterns were obtained by using a Siemens D-5000 X-ray diffractometer, employing Cu Kα radiation ($\lambda = 1.541$ Å) and settings of 40 kV and 20 mA.

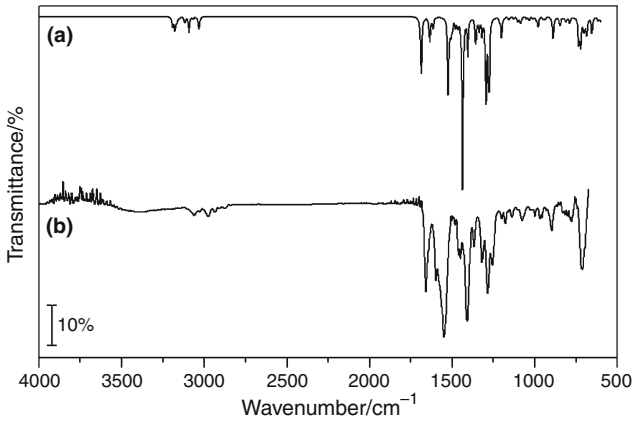

Fig. 3 Comparison between FTIR spectra of: theoretical (**a**) and experimental (**b**) of the La$(L)_3$

The attenuate total reflectance infrared spectra for ketoprofen sodium salt and for its metal-ion compounds were run on a Nicolet iS10 FTIR spectrophotometer, using an ATR accessory with Ge window, within the 4000–600 cm^{-1} range.

Computational strategy

In this study, the employed quantum chemical approach to determine the molecular structures was Becke three-parameter hybrid theory [18] using the Lee–Yang–Par (LYP) correlation functional [19], and the basis sets used for calculations were: 4 s for H (^{2}S) [20], [5s4p] for C (^{3}P) and O (^{3}P) [20], and [17s11p7d] for La (^{2}D) [21]. The diffuse functions for the lanthanum atom (^{2}D) were

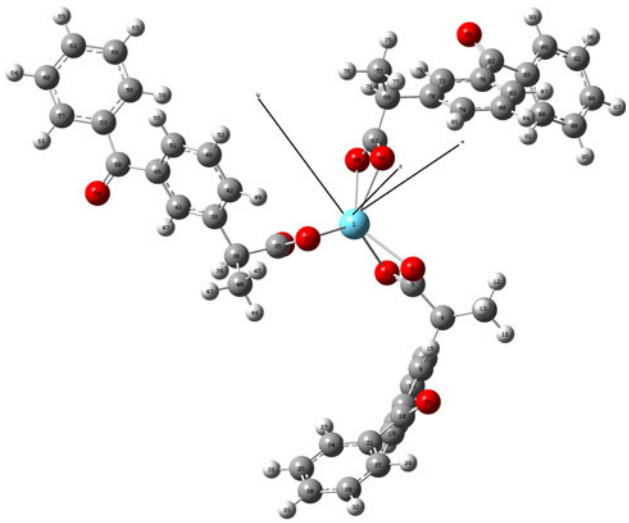

Fig. 4 Proposed theoretical structure 3D of solid-state anhydrous compound of lanthanum ketoprofen (optimized using DFT/B3LYP method)

Table 3 Theoretical data of structure 3D of solid-state anhydrous compound of lanthanum ketoprofen (optimized using DFT/B3LYP method)

Ato no.	Atom symbol	NA	NB	NC	Bond/Å	Angle/°	Dihedral/°	*X*/Å	*Y*/Å	*Z*/Å
1	La							0.07669	−0.24993	0.03313
2	0	1			2.48489			0.79217	−2.05843	−1.51352
3	C	2	1		1.28017	93.56779		0.81836	−2.94609	−0.59146
4	C	3	2	1	1.51962	119.3704	177.89152	1.16704	−4.38144	−0.9484
5	0	3	2	1	1.27877	120.14814	−0.85206	0.52968	−2.62933	0.61336
6	C	4	3	2	1.52446	108.83282	−92.71453	−0.12174	−5.14558	−1.22965
7	H	4	3	2	1.09129	105.64586	22.42924	1.72515	−4.32467	−1.88447
8	C	4	3	2	1.53395	111.81352	141.68063	2.03415	−5.04256	0.1305
9	C	6	4	3	1.39302	121.32321	−70.10076	−1.01577	−5.45842	−0.20821
10	C	6	4	3	1.39761	120.06869	110.16887	−0.42459	−5.55248	−2.53197
11	H	8	4	3	1.09128	110.00127	−179.62683	2.27209	−6.06771	−0.15821
12	H	8	4	3	1.09239	110.78429	−59.86399	2.97091	−4.49655	0.26334
13	H	8	4	3	1.08926	111.33548	60.07915	1.52243	−5.06441	1.09183
14	C	9	6	4	1.39828	121.10578	179.4273	−2.20232	−6.14916	−0.47314
15	H	9	6	4	1.08218	120.64037	−0.35384	−0.8092	−5.16817	0.81365
16	C	10	6	4	1.39063	120.82923	179.41517	−1.58985	−6.26083	−2.8045
17	H	10	6	4	1.08433	119.505	−0.26991	0.26104	−5.3166	−3.33822
18	C	14	9	6	1.49687	117.93926	177.44669	−3.08344	−6.49953	0.68509
19	C	16	10	6	1.38965	120.15546	1.20356	−2.48469	−6.55262	−1.78212
20	H	16	10	6	1.08349	119.88075	−178.7314	−1.79936	−6.58659	−3.8164
21	C	18	14	9	1.49483	120.53458	150.79247	−4.56249	−6.61993	0.50499
22	0	18	14	9	1.22775	119.65189	−29.26848	−2.58566	−6.69036	1.79105
23	H	19	16	10	1.08228	119.8785	−179.196	−3.38382	−7.11544	−1.99689
24	C	21	18	14	1.39903	122.65391	−30.83286	−5.27191	−5.86758	−0.43734
25	C	21	18	14	1.40022	118.17205	152.69623	−5.26653	−7.46903	1.36752
26	C	24	21	18	1.39126	120.38546	−176.52552	−6.65756	−5.9643	−0.51617
27	H	24	21	18	1.08253	119.99972	1.89435	−4.74533	−5.18625	−1.09338
28	C	25	21	18	1.38755	120.45383	177.8392	−6.64612	−7.58223	1.27167
29	H	25	21	18	1.08232	118.63059	−2.05169	−4.71262	−8.03095	2.10836
30	C	26	24	21	1.39133	120.06284	−0.99383	−7.34526	−6.82792	0.3306
31	H	26	24	21	1.08349	119.80761	179.01475	−7.19903	−5.3654	−1.23873
32	H	28	25	21	1.08358	119.89106	179.11289	−7.18024	−8.25292	1.93427
33	H	30	26	24	1.08378	120.02203	−179.3577	−8.42369	−6.91046	0.26155
34	O	1	2	3	2.47971	102.02485	−126.46211	−1.94366	0.63182	−1.1025
35	C	34	1	2	1.28031	93.84818	129.90661	−2.66838	0.56993	−0.04886
36	C	35	34	1	1.51848	119.50828	177.16917	−4.10161	1.06928	−0.09651
37	O	35	34	1	1.27948	120.05112	−1.53997	−2.17723	0.11307	1.04069
38	C	36	35	34	1.52457	109.26005	−95.26019	−4.14843	2.51118	0.3965
39	H	36	35	34	1.09079	105.89207	20.2963	−4.3817	1.07306	−1.15071
40	C	36	35	34	1.53522	111.6463	139.67588	−5.0481	0.14961	0.68787
41	C	38	36	35	1.39069	120.03388	117.86174	−4.57296	3.52478	−0.45579
42	C	38	36	35	1.39987	121.30695	−63.25413	−3.79227	2.8431	1.70899
43	H	40	36	35	1.09119	109.90787	−178.8357	−6.07118	0.52256	0.61786
44	H	40	36	35	1.09233	110.95814	−59.01242	−5.02456	−0.86702	0.289
45	H	40	36	35	1.08958	111.14399	60.96802	−4.76762	0.10193	1.73966
46	C	41	38	36	1.39965	121.34172	179.80822	−4.6304	4.85706	−0.03066
47	H	41	38	36	1.08294	120.40332	0.04263	−4.87263	3.29733	−1.47129
48	C	42	38	36	1.38956	120.54399	−178.9123	−3.8623	4.15954	2.14826
49	H	42	38	36	1.08352	119.67451	1.33563	−3.45554	2.06704	2.386
50	C	46	41	38	1.49631	117.9618	−177.34486	−5.15576	5.87774	−0.99043

Table 3 continued

Ato no.	Atom symbol	NA	NB	NC	Bond/Å	Angle/°	Dihedral/°	*X*/Å	*Y*/Å	*Z*/Å
51	C	48	42	38	1.39141	120.37561	−0.84433	−4.27131	5.16927	1.28272
52	H	48	42	38	1.08357	119.78222	179.06651	−3.59814	4.40036	3.17117
53	C	50	46	41	1.49471	120.58268	−151.48983	−4.6959	7.29807	−0.91728
54	O	50	46	41	1.22809	119.63128	28.58546	−5.97297	5.54429	−1.84434
55	H	51	48	42	1.08225	119.85284	179.03778	−4.33775	6.18934	1.63811
56	C	53	50	46	1.39897	122.66933	31.2426	−3.41375	7.65547	−0.48663
57	C	53	50	46	1.40026	118.14509	−152.33925	−5.56557	8.29803	−1.36951
58	C	56	53	50	1.39126	120.37751	176.52432	−3.01096	8.98702	−0.50538
59	H	56	53	50	1.08245	119.9981	−1.75443	−2.71907	6.89122	−0.16254
60	C	57	53	50	1.38754	120.44603	−177.82733	−5.17044	9.62811	−1.36538
61	H	57	53	50	1.08232	118.64347	2.06527	−6.54765	8.01087	−1.72232
62	C	58	56	53	1.39129	120.06788	0.9662	−3.89082	9.97546	−0.93495
63	H	58	56	53	1.08348	119.79838	−178.94213	−2.00994	9.2513	−0.18594
64	H	60	57	53	1.0836	119.89217	−179.12474	−5.85577	10.39612	−1.70401
65	H	62	58	56	1.0838	120.02673	179.38676	−3.57971	11.01363	−0.93989
66	O	1	34	35	2.47685	104.09082	−123.72476	1.79327	1.49402	−0.34998
67	C	66	1	34	1.28068	94.0074	127.94379	2.10071	1.59081	0.88947
68	C	67	66	1	1.51865	119.47195	176.68845	3.22795	2.51773	1.3095
69	O	67	66	1	1.27889	120.07358	−1.93138	1.47878	0.89085	1.76058
70	C	68	67	66	1.52446	109.24508	−95.40007	4.51928	1.71639	1.42906
71	H	68	67	66	1.09082	105.9269	20.18209	3.35479	3.22558	0.48929
72	C	68	67	66	1.53518	111.62651	139.5212	2.88554	3.27667	2.59929
73	C	70	68	67	1.39081	120.0414	117.97218	5.60371	2.01741	0.6119
74	C	70	68	67	1.39994	121.31198	−63.05227	4.65148	0.68523	2.36664
75	H	72	68	67	1.09116	109.91767	−179.12337	3.70605	3.94446	2.86663
76	H	72	68	67	1.09242	110.89975	−59.34524	1.98198	3.87688	2.47009
77	H	72	68	67	1.08964	111.13507	60.65165	2.7145	2.58838	3.42653
78	C	73	70	68	1.39962	121.3475	179.93128	6.80258	1.30048	0.69951
79	H	73	70	68	1.08297	120.38942	0.10854	5.53859	2.82131	−0.11082
80	C	74	70	68	1.38951	120.54432	−179.00158	5.84295	−0.02131	2.47597
81	H	74	70	68	1.08351	119.72777	1.30896	3.8162	0.43269	3.00892
82	C	78	73	70	1.49629	117.99676	−177.42284	7.94055	1.72541	−0.17418
83	C	80	74	70	1.39132	120.384	−0.88042	6.91594	0.275	1.64132
84	H	80	74	70	1.08357	119.77439	179.07844	5.93659	−0.80708	3.2162
85	C	82	78	73	1.49476	120.54444	−151.0173	8.95667	0.73087	−0.63538
86	O	82	78	73	1.22802	119.65105	28.98688	8.03921	2.90128	−0.51423
87	H	83	80	74	1.0823	119.83684	179.10501	7.84474	−0.27108	1.74386
88	C	85	82	78	1.39898	122.60458	31.10134	8.64623	−0.61433	−0.86167
89	C	85	82	78	1.40021	118.20216	−152.51911	10.24889	1.18869	−0.92025
90	C	88	85	82	1.39121	120.37549	176.47973	9.61033	−1.48453	−1.36039
91	H	88	85	82	1.08242	119.98953	−1.8115	7.64368	−0.97709	−0.67475
92	C	89	85	82	1.38757	120.44329	−177.7837	11.21581	0.31419	−1.39528
93	H	89	85	82	1.08232	118.63822	2.09804	10.47449	2.23565	−0.764
94	C	90	88	85	1.39125	120.06844	0.96521	10.89774	−1.02464	−1.61858
95	H	90	88	85	1.0835	119.80578	−178.96653	9.35518	−2.52071	−1.54802
96	H	92	89	85	1.08359	119.8935	−179.11494	12.21699	0.67506	−1.59921
97	H	94	90	88	1.0838	120.02768	179.37846	11.65104	−1.70547	−1.99757

Atom No. + *NA* bond, *Atom No.* + *NA* + *NB* angle; *Atom No.* + *NA* + *NB* + *NC* dihedral, *XYZ* cartesian coordinate

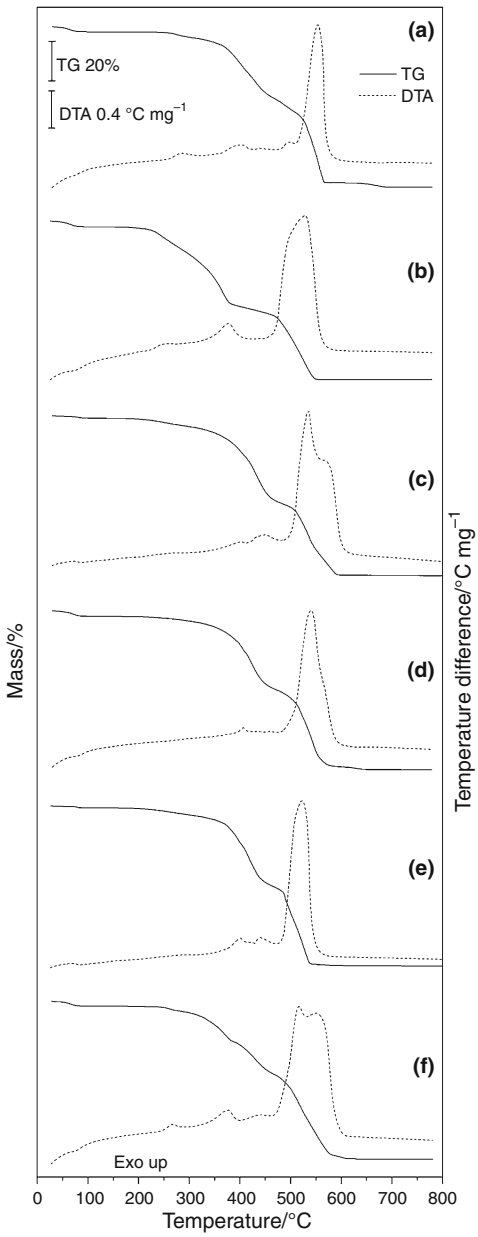

Fig. 5 TG–DTA curves of the compounds **a** $La(L)_3{\cdot}1H_2O$ (m = 4.970 mg), **b** $Ce(L)_3{\cdot}1.5H_2O$ (m = 4.760 mg), **c** $Pr(L)_3{\cdot}0.5H_2O$ (m = 5.054 mg), **d** $Nd(L)_3{\cdot}1.5H_2O$ (m = 5.069 mg), **e** $Sm(L)_3{\cdot}0.5H_2O$ (m = 5.081 mg), **f** $Eu(L)_3{\cdot}1H_2O$ (m = 4.948 mg)

calculated according to the procedure described in Ref. [21] and these values are: $\alpha s = 0.00669534$, $\alpha p = 0.079333735$, $\alpha d = 0.096432865$. In order to better describe the properties of the compound in the implementation of the calculations, it was necessary to include polarization functions [22] for all atoms of the compounds. The polarization functions are: $\alpha p = 0.33353749$ for H (^2S), $\alpha d = 0.72760279$, and $\alpha d = 0.36059494$ for C (^3P) and O (^3P), respectively, and $\alpha f = 0.36935391$ for La (^2D) atoms. The role of a basis set is a crucial point in theoretical studies of metal complexes, since the description of the configuration of the metal in the complex differs from the neutral state. The performed molecular calculations in this study were done using the Gaussian 09 routine [23].

The theoretical infrared spectrum, it was calculated using a harmonic field [24] based on C_1 symmetry (electronic state ^1A). Frequency values (not scaled), relative intensities, assignments, and description of vibrational modes are presented. The geometry optimization was computed using the optimized algorithm of Berny [25] and the calculations of vibrational frequencies were also implemented to determine an optimized geometry constitutes minimum or saddle points. The principal infrared-active fundamental modes assignments and descriptions were done by the GaussView 5.0.2 W graphics routine [26].

Results and discussion

The analytical results from TG and complexometry are shown in Table 1. These data permitted to establish the stoichiometry of the compounds, which is in agreement with general formula $Ln(L)_3{\cdot}nH_2O$, where Ln represents lighter lanthanides (La-Eu), L is ketoprofen and n = 1 (La, Eu), 1.5 (Ce, Nd), and 0.5 (Pr, Sm).

The X-ray powder patterns showed that all the compounds were obtained with low crystallinity degree and without evidence for the formation of an isomorphous series.

Infrared spectroscopic data on ketoprofen (sodium salt) and its compounds with La, Ce, Pr, Nd, Sm, and Eu are shown in Table 2 and Fig. 2. The bands found for ketoprofen (sodium salt) are centered at 1660, 1645 cm^{-1} (ketonic carbonyl stretches), 1567 cm^{-1} (asymmetrical carboxylate vibration), and 1394 cm^{-1} (symmetrical carboxylate vibration). The ketonic carbonyl stretches vibrations frequency is unchanged in the compounds in comparison with sodium salt ($\sim$1658 cm^{-1}). These data suggest that the ketonic carbonyl does not participate in coordination with the metal centers.

The calculated values of (delta) (asymmetrical–symmetrical carboxylate vibrations) for the synthesized compounds, shows smaller values in comparison of those values calculated for the sodium salt (Table 2). These results suggest that the coordination of the metals occurs in the carboxylate site of ketoprofen as bidentate bond [27]. The great similarity between the spectra of the complexes suggests that all are coordinated in the same way. The theoretical calculations of infrared and 3D structure are in agreement with this interpretation (Figs. 3, 4). The theoretical infrared spectra for $La(L)_3$ (Fig. 3) are centered at

Table 4 Temperature ranges 9, mass losses and peak temperatures observed for each step of the TG–DTA curves of the compounds

Compounds		Steps			
		First	Second	Third	Fourth
$La(L)_3 \cdot lH_2O$	θ °C	30–100	243–457	457–584	616–700
	Loss/%	2.17	32.67	45.33	2.12
	Peak/°C	73 (endo)	283 and 397 (exo)	497 and 554 (exo)	
$Ce(L)_3 \cdot 1.5H_2O$	θ °C	30–100	161–390	390–566	
	Loss/%	3.06	40.05	38.27	
	Peak/°C	73 (endo)	249 and 377 (exo)	528 (exo)	
$Pr(L)_3 \cdot 0.5H_2O$	θ °C	30–100	191–472	472–613	–
	Loss/%	1.06	42.60	38.41	
	Peak/°C	88 (endo)	362–460 (exoterm)	535	
$Nd(L)_3 \cdot 1.5H_2O$	θ °C	30–100	212–461	461–587	587–654
	Loss/%	2.88	36.33	40.70	1.65
	Peak/°C	80 (endo)	406 (exo)	541 (exo)	
$Sm(L)_3 \cdot 0.5H_2O$	θ °C	30–100	206–460	460–600	–
	Loss/%	1.02	39.50	41.65	
	Peak/°C	84 (endo)	357–457 (exoterm)	523 (exo)	
$Eu(L)_3 \cdot lH_2O$	θ °C	30–100	200–388	388–465	465–630
	Loss/%	2.34	18.28	16.44	43.94
	Peak/°C	80 (endo)	266 and 375 (exo)	410–455 (exoterm)	518 (exo)

L ketoprofen

1688 cm^{-1} (ketonic carbonyl stretches), 1524 cm^{-1} (asymmetrical carboxylate vibration), and 1436 cm^{-1} symmetrical carboxylate vibration). The Table 3 showed the theoretical data of 3D structure of $La(L)_3$.

The simultaneous TG–DTA curves of the compounds are shown in Fig. 5, and the details of the thermal events (mass losses, temperature intervals, and peak temperatures) are described in Table 4. The TG curves exhibit mass losses in three (Ce, Pr, Sm) and four (La, Nd, Eu) steps and thermal events corresponding to these losses (DTA).

The first mass loss from 30 to 100 °C for all the compounds is attributed to dehydration, which occurs in a single step and TG curves show that the anhydrous compounds are stable up to 243 °C (La), 212 °C(Nd), 206 °C(Sm), 200 °C(Eu), 191 °C(Pr), and 161 °C(Ce). After dehydration, the mass losses observed for all the compounds are due to the thermal decomposition of organic ligand. These take place in consecutive and/or overlapping steps with partial losses which are characteristic for each compound.

For the anhydrous cerium, praseodymium, and samarium compounds, the thermal decomposition occurs in two steps. The first step is attributed to the decomposition of organic ligand. Small exothermic peaks corresponding to this loss are observed in DTA curve, probably due to endothermic and exothermic reactions must be occurring simultaneously (Fig. 5). The second step is attributes to the oxidation of the organic matter and it is accompanied by exothermic event in the DTA curve.

For the anhydrous lanthanum, neodymium, and europium compounds, the thermal decomposition occurs in three steps. The first and second steps are ascribed to the decomposition of organic ligand, Small exothermic peaks corresponding to this loss are observed in DTA curve, probably due to endothermic and exothermic reactions must be occurring simultaneously (Fig. 5).

The third step is attributes to the oxidation of the organic matter and it is accompanied by exothermic event in the DTA curves.

For all compounds, the final thermal decomposition residues were the respective oxides, CeO_2, Pr_6O_{11}, and Ln_2O_3 (Ln = La, Nd, Sm, and Eu) as proven by X-ray powder diffractometry.

The DSC curves of the compounds are shown in Fig. 6. These curves show endothermic and exothermic peaks that all are in accordance with the mass losses observed in the TG curves. The endothermic peaks at 85 °C (La), 80 °C (Ce, Pr, Sm), and 75 °C (Nd, Eu) are assigned to the dehydration. The dehydration enthalpies found for these compounds (La, Ce, Pr, Nd, Sm, and Eu) were 15.88, 33.36, 9.01, 52.50, 22.98, and 52.27 J g^{-1}, respectively.

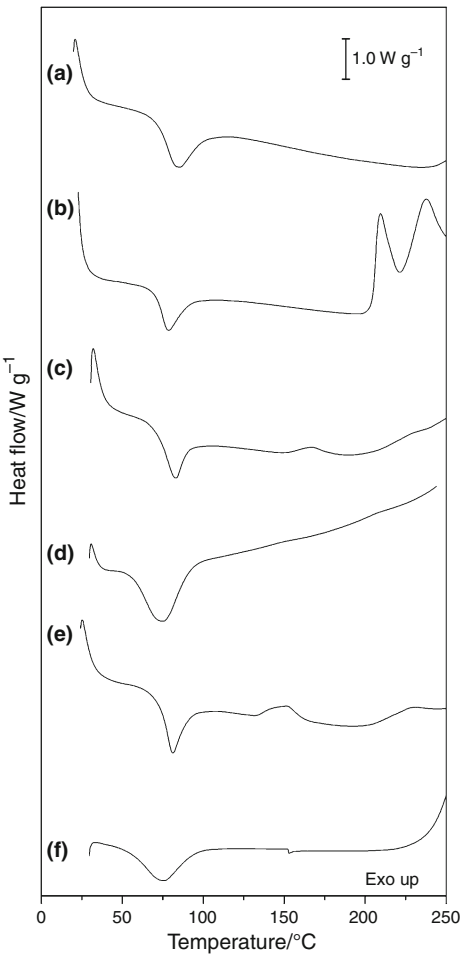

Fig. 6 DSC curves of the compounds **a** $La(L)_3{\cdot}1H_2O$ ($m = 3.10$ mg), **b** $Ce(L)_3{\cdot}1.5H_2O$ ($m = 2.98$ mg), **c** $Pr(L)_3{\cdot}0.5H_2O$ ($m = 3.40$ mg), **d** $Nd(L)_3{\cdot}1.5H_2O$ ($m = 3.56$ mg), **e** $Sm(L)_3{\cdot}0.5H_2O$ ($m = 3.08$ mg), **f** $Eu(L)_3{\cdot}1H_2O$ ($m = 2.95$ mg)

Conclusions

Based on the TG curves and the results of complexometric titration, a general formula could be established for the synthesized compounds. For all the compounds the TG curves show that the dehydration occurs in a single step and in the same temperature range. These curves also show that the thermal stability of the anhydrous compounds is characteristic of each compound. TG–DTA and DSC provided previously unreported information concerning the thermal behavior and thermal decomposition of these compounds.

The spectroscopic infrared experimental data and the theoretical calculations, suggests that the carboxylate of ketoprofen is coordinate to metals as bidentate bond and the great similarity between the infrared experimental spectra of the complexes suggests that all are coordinated in the same way.

Acknowledgements The authors thank to FAPESP (Proc. 2010/10931-3), FUNDUNESP, PROPe-UNESP, CNPq Foundations (Brazil) for financial support and Prof. Dr. Massao Ionashiro, for permitting the use of his TG–DTA equipment from TA instruments. This research was supported by resources supplied by the Center for Scientific Computing (NCC/GridUNESP) of the Sao Paulo State University (UNESP), Instituto de. Quimica de Araraquara, UNESP Campus de Araraquara and CENAPAD-UNICAMP.

References

1. Noordin MI, Chung LY. Thermostability and polymorphism of theobroma oil and palm kernel oil as suppository bases. J Therm Anal Calorim. 2009;95:891–4.
2. Campanella L, Micieli V, Tomassetti M, Vecchio S. Quantitative determination of acetylsalicylic acid in commercial drugs using DSC Comparison with titration and UV spectrophotometric methods. J Therm Anal Calorim. 2010;102:249–59.
3. Bannach G, Arcaro R, Ferroni DC, Siqueira AB, Treu-Filho O, Ionashiro M, Schnitzler E. Thermoanalytical study of some anti-inflammatory analgesic agents. J Therm Anal Calorim. 2010;102:163–70.
4. Bruni G, Berbenni V, Milanese C, Girella A, Marini A. Drug-excipient compatibility studies in binary and ternary mixtures by physico-chemical techniques. J Therm Anal Calorim. 2010;102:499–503.
5. Neto HS, Novak C, Matos JR. Thermal analysis and compatibility studies of prednicarbate with excipients used in semi solid pharmaceutical form. J Therm Anal Calorim. 2009;97:367–74.
6. Krupaa A, Majdab D, Jachowicza R, Mozgawac W. Solid-state interaction of ibuprofen and Neusilin US2. Thermochim Acta. 2010;509:12–7.
7. Miltykb W, Antonowiczb E, Komstaa L. Recognition of tablet content by chemometric processing of differential scanning calorimetry curves—an acetaminophen example. Thermochim Acta. 2010;508:146–9.
8. Giron D, Monnier S, Mutz M, Piechon P, Buser T, Stowasser F, Schulze K, Bellus M. Comparison of quantitative methods for analysis of polyphasic pharmaceuticals. J Therm Anal Calorim. 2007;89:729–43.
9. Bannach G, Cervini P, Cavalheiro ETG, Ionashiro M. Using thermal and spectroscopic data to investigate the thermal behavior of epinephrine. Thermochim Acta. 2010;499:123–7.
10. Giron D. Applications of thermal analysis and coupled techniques in pharmaceutical industry. J Therm Anal Calorim. 2002;68:335–57.
11. Mura P, Mandersioli A, Bramanti G, Furlanetto S, Pinzauti S. Utilization of differential scanning calorimetry as a screening technique to determine the compatibility of ketoprofen with excipients. Int J Pharm. 1995;119:71–9.
12. Botteghi C, Marchetti M, Del Ponte G. Contribuições recentes da reação de hidroformilação na síntese de produtos farmacêuticos. Parte II Quim Nova. 1997;20:30–48.
13. Heffeter P, Jakupec MA, Körner W, Wild S, von Keyserlingk NG, Elbling L, Zorbas H, Korynevska A, Knasmüller S, Sutterlüty H, Micksche M, Keppler BK, Berger W. Anticancer activity of the lanthanum compound [tris(1,10-phenanthroline)lanthanum(III)]trithiocyanate (KP772; FFC24). Biochem Pharmacol. 2006;71:426–40.
14. Kostova I, Trendafilova N, Momekov G. Theoretical, spectral characterization and antineoplastic activity of new lanthanide complexes. J Trace Elem Med Biol. 2008;22:100–11.
15. Sessler JL, Dow WC, Connor DO, Harriman A, Hemmi G, Mody TD, Miller RA, Qing F, Springs S, Woodburn K, Young KW.

Biomediacal applications of lanthanide (III) texaphyrins Lutetium (III) texaphyrins as potential photodynamic therapy photosensitizers. J Alloys Compd. 1997;249:146–52.
16. Yam VWW, Lo KKW. Recent advances in utilization of transition metal complexes and lanthanides as diagnostic tools. Coord Chem Rev. 1998;184:157–240.
17. Flaschka HA. EDTA Titrations. Oxford: Pergamon Press; 1964.
18. Becke AD. Density-functional thermochemistry.3. The role of exact exchange. J Chem Phys. 1993;98:5648–52.
19. Lee C, Yang W, Parr RG. Development of the colle-salvetti correlation-energy formula into a functional of the electron-density. Phys Rev B. 1988;37:785–9.
20. Treu-Filho O, Pinheiro JC, da Costa EB, Ferreira JEV, de Figueiredo AF, Kondo RT, de Lucca Neto VA, de Souza RA, Legendre AO, Mauro AE. Experimental and theoretical study of the compound [Pd(dmba)(NCO)(imz)]. J Mol Struct. 2007;829: 195–201.
21. Treu Filho O, Pinheiro JC, Kondo RT, Marques RFC, Paiva-Santos CO, Davolos MR, Jafelicci M Jr. Gaussian basis sets to the theoretical study of the electronic structure of perovskite ($LaMnO_3$). J Mol Struc (Theochem). 2003;631:93–9.
22. Oswaldo TF, Ciriaco PJ, Toshiaki KR. Designing Gaussian basis sets to the theoretical study of the piezoelectric effect of perovskite ($BaTiO_3$). J Mol Struct. 2004;671:71–5.
23. Gaussian 09, Revision **A.02**, Frisch MJ, Trucks GW, Schlegel HB, Scuseria GE, Robb, MA, Cheeseman JR, Scalmani G, Barone V, Mennucci B, Petersson GA, Nakatsuji H, Caricato M, Li X, Hratchian HP, Izmaylov AF, Bloino J, Zheng G, Sonnenberg JL, Hada M, Ehara M, Toyota K, Fukuda R, Hasegawa J, Ishida M, Nakajima T, Honda Y, Kitao O, Nakai H, Vreven T, Montgomery Jr. JA, Peralta JE, Ogliaro F, Bearpark M, Heyd JJ, Brothers E, Kudin KN, Staroverov VN, Kobayashi R, Normand J, Raghavachari K, Rendell A, Burant JC, Iyengar SS, Tomasi J, Cossi M, Rega N, Millam NJ, Klene M, Knox JE, Cross JB, Bakken V, Adamo C, Jaramillo J, Gomperts R, Stratmann RE, Yazyev O, Austin AJ, Cammi R, Pomelli C, Ochterski JW, Martin RL, Morokuma K, Zakrzewski VG, Voth GA, Salvador P, Dannenberg JJ, Dapprich S, Daniels AD, Farkas Ö, Foresman JB, Ortiz JV, Cioslowski J, Fox DJ. Gaussian, Inc., Wallingford CT, 2009.
24. Goodson DZ, Sarpal SK, Wolfsberg M. Influence on isotope effect calculations of the method of obtaining force constants from vibrational data. J Phys Chem. 1982;86:659–63.
25. Schelegel HB. In: Bertran J, editor. New theoretical concepts for understanding organic reactions. The Netherlands: Academic; 1989. p. 33–53.
26. GaussView, Version 5.0.8, Dennington, R.; Keith, T.; Millam, J. Semichem Inc., Shawnee Mission KS, 2000-2008.
27. Deacon GB, Phillips RJ. Relationships between the carbon–oxygen stretching frequencies of carboxylato complexes and the type of carboxylate coordination. Coord Chem Rev. 1980;33: 227–50.